

УДК 539.12

## STATUS OF THE EDELWEISS EXPERIMENT

*M.Stern*

Institut de Physique Nucléaire de Lyon and Université Claude Bernard, Lyon-1, IN2P3-CNRS, 43 Bd. du 11 novembre 1918, 69622 Villeurbanne Cedex, France

For the EDELWEISS collaboration<sup>1</sup>

The search for the nonbaryonic dark matter has become a very active research area. Possible candidates include WIMPs which could scatter on nuclei of the crystal producing nuclear recoils. The resulting ionization and heat are measured with a 70 g Ge detector. Preliminary results with a 320 g bolometer are also described in the prospect of the second stage of the EDELWEISS experiment.

Поиск темной материи становится очень активной областью исследования. К возможным кандидатам относятся слабовзаимодействующие массивные частицы (WIMPs), в результате рассеяния которых на ядрах кристалла образуются ядра отдачи. Ионизационные и тепловые сигналы регистрируются Ge-детектором с массой 70 г. В работе также представлены предварительные результаты второй стадии эксперимента EDELWEISS с болометром массой 320 г.

### INTRODUCTION

The search for dark matter has become a very active research area. There is evidence that a large part of the dark matter in the universe is non baryonic [1]. Theoretical models provide a wide selection of possible candidates including particles called WIMPs (Weakly Interacting Massive Particles) with mass more than some tens of  $\text{GeV}/c^2$ . The EDELWEISS experiment is dedicated to the detection of nuclear recoils from elastic scattering with these particles. We intend to detect the recoils in a direct way with a double signal of heat and ionization. The experimental set-up of EDELWEISS I stage has been described elsewhere [2]. The method requires a cryogenic detector with good performances, sensitive to the expected very small temperature variations. Taking into account the expected small energy depositions and the very low rates, the method is very sensitive to cosmic rays and to the background radioactive environment. For this reason, the experimental set-up is located in the Fréjus underground laboratory at the border between France and Italy and it is carefully shielded against radioactivity.

### 1. PRINCIPLE

A WIMP produces an elastic scattering on a germanium nucleus as displayed on Fig. 1. For natural germanium the cross section of the reaction is essentially governed by a scalar coupling connected to the nucleus mass and leads to event rates of  $< 1 \text{ evt/day/kg}$  in the frame of the Minimal SuperSymmetric Models (MSSM) [3] compatible with other existing data.

---

<sup>1</sup>The full author list is given at the end of the paper.

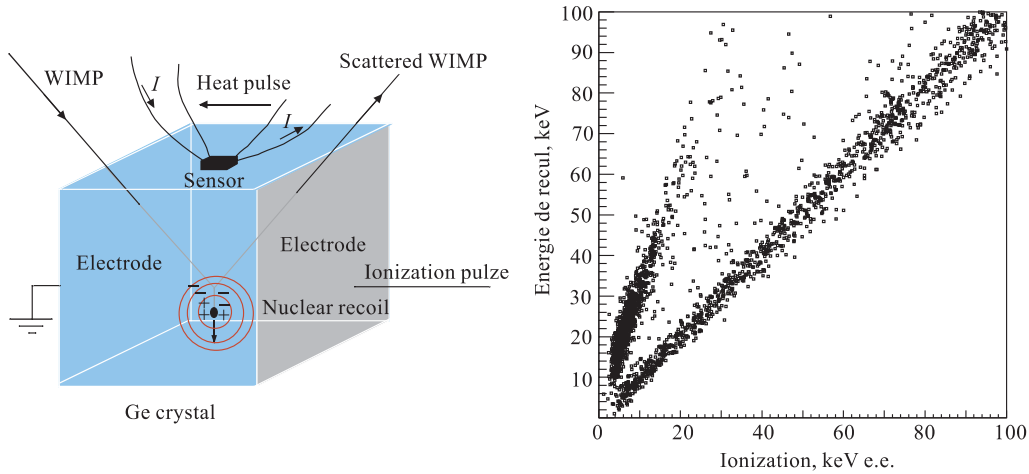


Fig. 1. A schematic view of the detector illustrating the double signal : heat, ionization

Fig. 2. Recoil energy versus ionization energy diagram; on the first diagonal, the photon calibration can be seen and the upper line corresponds to nuclear recoils obtained with a neutron source

The EDELWEISS detector is sensitive to a nuclear recoil above  $\geq 10$  keV, and thus of galactic halo WIMPs with masses of some tens of GeV and a mean velocity of about 300 km/s. The nuclear recoil leads to the ionization in the crystal along the trajectory of the nucleus together with a heating of the crystal. The heat generated during the charge transport to the electrodes, the Luke–Neganov effect [4], must be subtracted from the phonon amplitude to recover the recoil energy. In the same way, gammas and  $\beta$ 's of the radioactive background produce electronic recoils. Figure 2 displays the ionization versus phonon scatter diagram. By convention the gamma events give the same amount of both types of energies and therefore the corresponding events are located along the first diagonal on Fig. 2. On the contrary nuclear recoils induced by neutrons produce around 3 times less ionization and the corresponding events are located on the upper line. The different slopes of the two lines allow us to reject 99 % of the electron recoils which constitute most of the radioactive background. Neutrons of a few MeV and WIMPs both produce nuclear recoils and therefore have the same signature on this diagram.

## 2. EDELWEISS I-SYNTHESIS OF FIRST RESULTS

**2.1. Bolometer Characteristics.** The first of the EDELWEISS detectors, a 70 g germanium bolometer studied more extensively in L'Hôte et al. [5], is displayed on Fig. 3. The electrodes are made of boron and phosphorus implantation at low energy (typically between 5 and 15 keV) to obtain very thin electrodes with very steep profiles. A p-i-n structure is created allowing large electric fields.

The thermometer is a NTD (Neutron Transmutation Doped) sensor. These sensors are made of germanium strongly doped by thermal neutrons. The doping rate is calculated in order to get semiconductors close to the metal-insulator transition. The upper and lower faces

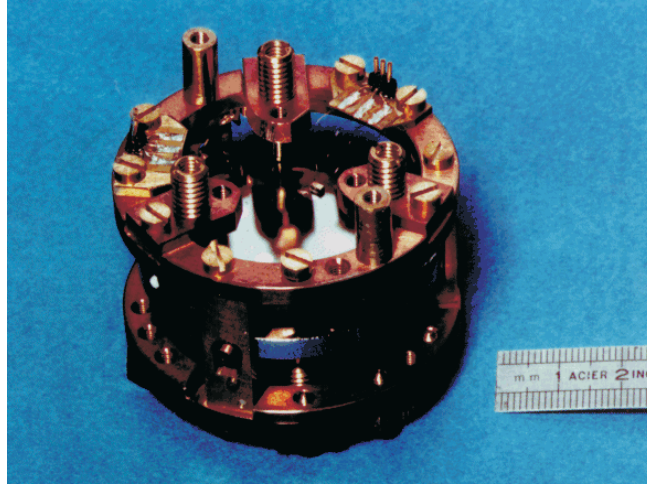


Fig. 3. A high purity 70 g Ge bolometer in its copper holder ( $h = 8$  mm,  $\Phi = 48$  mm)

of the thermometer are metallized on a depth of some tens of nm and the thermometer is glued by Epotek to one electrode of the detector assuring a thermal and electrical contact. Performances of this detector in calibration runs with a  $^{57}\text{Co}$  source ( $E_\gamma = 122$  keV) at typical temperatures between 10 and 20 mK are:

Ionization measurement:  $\approx 1$  keV resolution FWHM.

Heat measurement:  $\Delta T \approx 0.1 \mu\text{K/keV} \rightarrow \approx 1$  keV resolution FWHM.

As noted previously the heat signal incorporates an amplitude proportional to the polarisation. Therefore the measured heat is a function of the bias voltage applied to the electrodes. By convention, charge and initial phonon amplitudes are normalized with respect to electron recoils from a gamma ray source. The heat can be connected to the ionization according to the formula (1):

$$\text{Heat} = (\text{Recoil} + (V/3) \text{ Ionization}) / (1 + V/3). \quad (1)$$

Once corrected for the Luke–Neganov effect, the ratio of ionization to recoil energy is a direct measurement of quenching factor in Ge and is almost completely independent of the applied voltage as displayed on Fig. 2.

**2.2. Set-Up Environment — Set-Up Upgrade.** Several measurements of the background have been realized in the laboratory [6,7]. The following figures apply to the Fréjus Underground Laboratory (4600 m water. eq.): muon flux of  $4.6/\text{m}^2/\text{day}$ , 1–10 MeV neutron flux of  $0.4 \text{ n/cm}^2/\text{day}$ . Moreover the radioactive background of the bolometer mounting has been minimized. After a first commissioning run in 1997, the experimental set-up has been moved to an acoustically and electrically better isolated location as displayed on Fig. 4.

In the vicinity of the bolometer a shield of archeological lead has been introduced. In addition a removable 30 cm paraffin shield surrounds the installation and strongly reduces

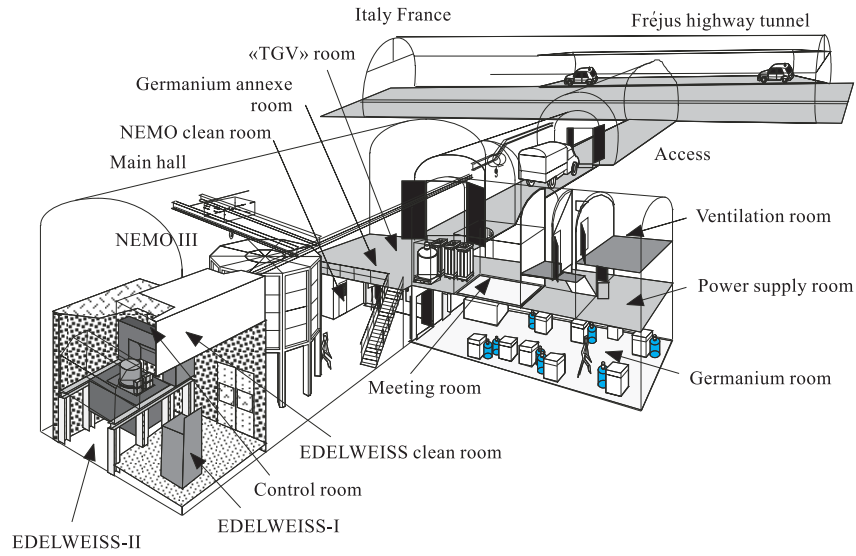


Fig. 4. View on the LSM (Laboratoire Souterrain de Modane). At the first stage, the space for the EDELWEISS experiment, at the last stage the highway tunnel

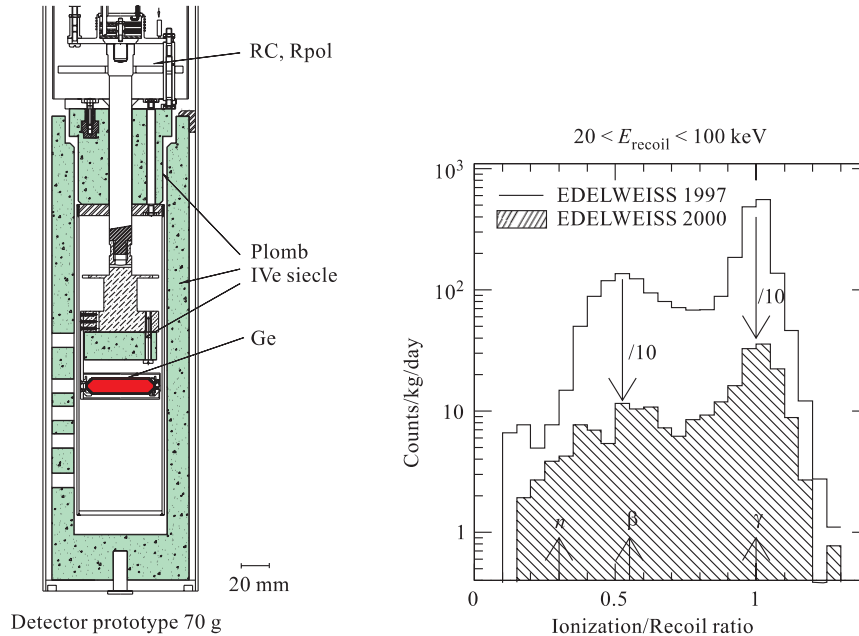


Fig. 5. Cryostat after the improvements of 1998 and 1999

Fig. 6. Number of counts/kg/day versus the Ionization/Recoil ratio. Evolution of the results with the upgrades: solid line — EDELWEISS, 1997; shaded region — EDELWEISS, 2000

the flux of MeV-range neutrons. A permanent nitrogen flushing protects the experimental set-up from radon. Furthermore, concerning the bolometer itself, a new implantation profile of  $B$  and  $P$  for the electrodes has been tested, and the front-end electronics has been moved beyond the Roman lead shielding (Fig. 5).

**2.3. New results.** The quality of the results largely justifies these improvements as illustrated by Fig. 6. The results correspond to an exposure of 1.8 kg-day before the upgrade and 3.2 kg-day after. The Figure displays the number of events/day/kg versus the ionization/recoil  $R$  ratio which is expected to vary between  $\approx 0.3$  and  $\approx 1$  for nucleon and electron recoils, respectively. Three zones are differentiated. The comparison of the runs of 1997 and 2000 shows the population of the zone, called  $\gamma$  around the  $R$  value 1, has been divided by  $\approx 10$ , the population of the intermediate  $R$  values called  $\beta$  has been divided by  $\approx 10$  while the reduction of  $R$  is only  $\approx 2$  in the neutron zone. The intermediate zone corresponds to the electronic recoils with incomplete charge collection which are most probably due to  $\beta$  and or  $X$  interactions near the surface. Investigations are in progress to eliminate them. Nevertheless, the improvements are obvious, even if they don't concern the whole ratio spectrum in a uniform way.

### 3. BOLOMETER R & D

The performances of a bolometer are very dependent on the operating temperature since a deposited energy  $E$  induces a temperature variation  $\Delta T = E/C$ , where  $C$  is the total (absorber + sensor) specific heat involving the contributions of lattice and electrons, both depending on the temperature. Concerning the resistor sensors, two types of materials are adapted: the superconductors in the normal-superconductor transition zone and the semiconductors strongly doped close to the metal-insulator transition. As already mentioned we have adopted the second ones by choosing NTD sensors. The properties of such systems are those of properties of «Anderson insulators», or insulators in the vicinity of the insulator-metal transition. Another alternative to these glued NTD sensors is the direct deposition by evaporation of amorphous thin layers  $\text{Nb}_x\text{Si}_{1-x}$  on the chosen absorber. The properties of this system move between superconductivity and Anderson insulator according to the  $x$  value. The investigations concerning the abilities of thin layers are performed at the CSNSM [8,9]. One typical heat signal is displayed on Fig. 7. The amplitude of the signal is higher than the one expected in a bolometer working in thermal equilibrium. We observe two components, one fast and one slow. The first one is due to the ballistic phonons, while the second one is due to the thermal phonons. The two diagrams in Fig. 8 show the ionization amplitude versus the fast and the slow component in the heat channel, respectively, as measured in a  $^{57}\text{Co}$  source run. A larger spread of the events is observed with the fast component. This is due to the limited lifetime of the ballistic phonons, which leads to a decay of the fast component with increasing distance of the recoil

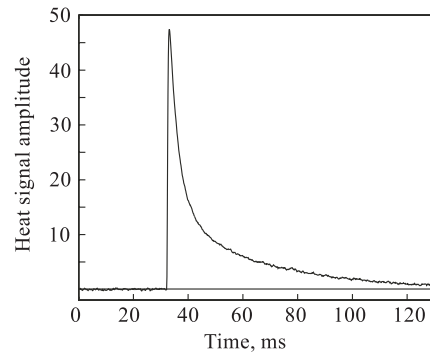


Fig. 7. Heat signal amplitude for a 16 g Ge bolometer equipped with a NbSi sensor

from the sensor. We will take advantage of this position sensitivity to separate surface events from bulk events and consequently to improve the discrimination.

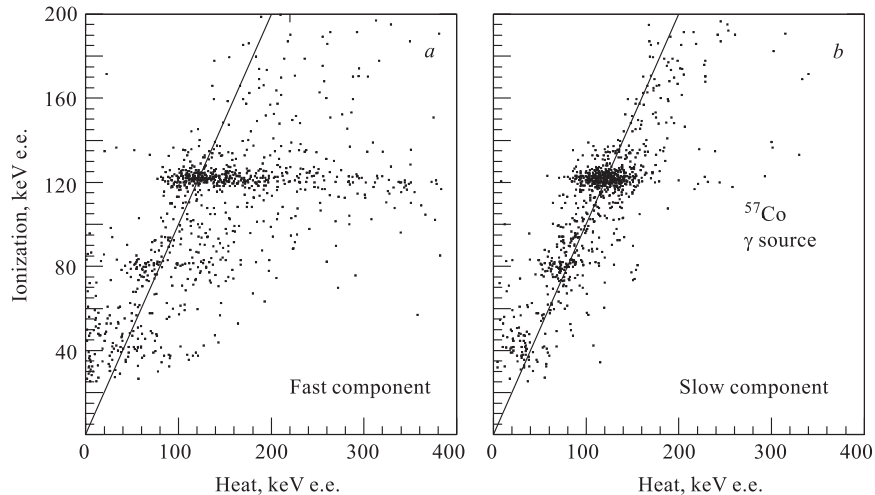


Fig. 8. Ionization versus heat diagrams. 16 g Ge bolometer equipped with a NbSi film sensor

Another development concerns the size of the absorber. Despite the reduction of the heat amplitude in the mass ratio, larger detectors increase the probability to observe the expected particles. A 320 g bolometer has been tested and already gives good results. This size of bolometers will be adopted for the next stage of the experiment.

#### 4. EDELWEISS-II STAGE

The available volume of the present cryostat in Modane (LSM) is about one liter. For the time being, two 320 g detectors are being tested. In the last phase of EDELWEISS I, data will be taken with  $3 \times 320$  g detectors. This is the maximal mass which can be hosted in the available volume. Then the EDELWEISS-II experiment will take place. The construction of a 100 l cryostat by the CRTBT in Grenoble is in progress. It is a dilution refrigerator with pulse tubes to avoid the use of nitrogen. Shieldings and muon veto are under study. The knowledge of the different components will determine the composition and the thicknesses of the adopted materials while respecting the constraints of available space and security. The new dedicated electronics will consist of cold front-end amplification and digitization modules mounted on the cryostat and input/output through optical fibre.

#### CONCLUSION

For the last two years the results have demonstrated the validity of the detection method we have chosen for the two stages of EDELWEISS. The results for the 1 kg detector step will be available within some months. The intermediate results displayed at this Conference

confirm the adequacy of this choice. The calibration of the recoil energies in the detector is described elsewhere [10,11]. The bolometers continue to benefit from the developments such as new sensors, different electrode implantation schemes and guard rings in order to reject the incomplete charge collection events. This should insure a sensitivity at least equivalent to the ones observed by experiments using other detection methods.

## REFERENCES

1. *Spergel D.* Some Outstanding Questions in Astrophysics. J.N. Bahcall & J.P. Ostriker, 1997.
2. *Drain D. et al.* // Phys. Rep. 1998. V. 307. P.297–300.
3. *Jungman G.* Supersymmetric Dark Matter // Phys. Rep. 1999. V. 267, No.5–6. P. 195–376.
4. *Luke P.N. et al.* Calorimetric Ionization Detector // Nucl. Instr. Meth. in Phys. Res. A. 1990. V. 289. P.406–409.
5. *L'Hôte D.* // J. Appl. Phys. 2000. V. 87. P. 1507.
6. *Berger Ch. et al.* Nucl. Instr. Meth. A. 1987. V.262. P.463-495; *Berger Ch. et al.* // Phys. Rev. D. 1989. V. 40, No. 7. P. 2163–2171.
7. *Chazal V. et al.* // Astropart. Phys. 1998. V.9. P. 163–172.
8. *Juillard A.* Thèse de Doctorat (Université Paris XI Orsay, 1999). Unpublished.
9. *Marnieros S.* Thèse de Doctorat (Université Paris XI Orsay, 1998). Unpublished.
10. *Di Stefano P. et al.* (EDELWEISS Collaboration) // Astropart. Phys. (in press).
11. *Simon E. et al.* (EDELWEISS Collaboration) (in preparation).

The EDELWEISS collaboration: A. Benoit<sup>a</sup>, L. Bergé<sup>b</sup>, A. Broniatowski<sup>b</sup>, B. Chambon<sup>c</sup>, M. Chapellier<sup>d</sup>, G. Chardin<sup>e</sup>, P. Charvin<sup>f</sup>, M. De Jésus<sup>c</sup>, P. Di Stefano<sup>e</sup>, D. Drain<sup>c</sup>, L. Dumoulin<sup>b</sup>, J. Gascon<sup>c</sup>, G. Gerbier<sup>e</sup>, C. Goldbach<sup>g</sup>, M. Goyot<sup>c</sup>, M. Gros<sup>e</sup>, J.-P. Hadjout<sup>c</sup>, S. Hervé<sup>e</sup>, A. Juillard<sup>b</sup>, A. de Lesquen<sup>e</sup>, M. Loidl<sup>e</sup>, J. Mallet<sup>e</sup>, M. Martin<sup>h</sup>, S. Marnieros<sup>b</sup>, O. Martineau<sup>c</sup>, N. Mirabolfati<sup>b</sup>, L. Mosca<sup>e</sup>, X.-F. Navick<sup>e</sup>, G. Nollez<sup>g</sup>, P. Pari<sup>d</sup>, C. Pastor<sup>c</sup>, E. Simon<sup>c</sup>, L. Vagneron<sup>c</sup>, D. Yvon<sup>e</sup>

<sup>a</sup> Centre de Recherche sur les Très Basses Températures(CRTBT), BP 166, 38042 Grenoble Cedex, France

<sup>b</sup> Centre de Spectroscopie Nucléaire et Spectrométrie de Masse (CSNSM) IN2P3-CNRS, Univ. Paris XI, bat. 108, 91405 Orsay Cedex, France

<sup>c</sup> Institut de Physique Nucléaire de Lyon and Université Claude Bernard, Lyon-1, IN2P3-CNRS, 43 Bd. du 11 novembre 1918, 69622 Villeurbanne Cedex, France

<sup>d</sup> Centre d'Etudes Nucléaires de Saclay(CEA), DSM/DRECAM/SPEC 91191 Gif-sur-Yvette Cedex, France

<sup>e</sup> Centre d'Etudes Nucléaires de Saclay(CEA), DSM/DAPNIA, 91191 Gif-sur-Yvette Cedex, France

<sup>f</sup> Laboratoire Souterrain de Modane(LSM), CEA-CNRS, 90 rue Polset, 73500 Modane, France

<sup>g</sup> Institut d'Astrophysique de Paris, INSU-CNRS, 98 bis Bd. Arago, 75014 Paris, France